MR. AZAM AHMED (Orcid ID : 0000-0002-1810-0427)

DR. SHIVA SHAHRARA (Orcid ID : 0000-0002-6698-8491)

IL-34 reprograms glycolytic and osteoclastic RA macrophages via Syndecan-1 and M-CSFR

Katrien Van Raemdonck Ph.D.,[1,2] Sadiq Umar Ph.D.,[1,2] Karol Palasiewicz B.S.,[1,2] Michael V. Volin Ph.D.,[3] Hatem A. Elshabrawy Ph.D.,[4] Bianca Romay B.S.,[2] Chandana Tetali B.S.,[2] Azam Ahmed,[2] M. Asif Amin M.D.,[5] Ryan K. Zomorrodi,[2] Nadera Sweiss M.D.,[2] Shiva Shahrara Ph.D.[1,2]*

[1] Jesse Brown VA Medical Center, Chicago, IL 60612, USA

[2] Department of Medicine, Division of Rheumatology, the University of Illinois at Chicago, IL 60612, USA

[3] Department of Microbiology and Immunology, Midwestern University, Downers Grove, IL 60515, USA

[4] Department of Molecular and Cellular Biology, College of Osteopathic Medicine, Sam Houston State University, Conroe, TX 77304, USA

[5] Division of Rheumatology, Clinical Autoimmunity Center of Excellence, University of Michigan Medical School, Ann Arbor, MI 48109, USA

*Corresponding author: Shiva Shahrara, Ph.D.

The University of Illinois at Chicago, Department of Medicine, Division of Rheumatology

840 S Wood Street, CSB suite 1114, Chicago, IL 60612

Telephone: (312) 413-7529

Fax: (312) 413-9271

E-mail: shahrara@uic.edu

Short title: IL-34 binding to SDC-1/M-CSFR rewires M34 MΦs

ABSTRACT

Objective: In RA, IL-34 serum levels are linked with increased disease severity. IL-34 binds to two receptors, M-CSFR and Syndecan-1 (SDC-1), which are co-expressed in RA macrophages (MΦs). Expression of both IL-34 and SDC-1 is strikingly elevated in the RA synovium, yet their mechanism of action remains undefined.

Methods: To characterize the significance of IL-34 in immunometabolism, its mechanism of action was elucidated in joint MΦs, fibroblasts and effector T cells using RA and preclinical models.

Results: Intriguingly, SDC-1 activates IL-34-induced M-CSFR phosphorylation and reprograms RA naïve cells into distinctive CD14$^+$CD86$^+$GLUT1$^+$M34 MΦs that express elevated levels of IL-1β, CXCL8 and CCL2. In murine M34 MΦs, the inflammatory phenotype is accompanied by potentiated glycolytic activity, exhibited by transcriptional upregulation of GLUT1, C-MYC and HIF1α and amplified pyruvate and L-lactate secretion. Local expression of IL-34 provokes arthritis, by expanding the glycolytic F4/80$^+$iNOS$^+$MΦ population, which in turn attracts

fibroblasts and polarizes Th1/Th17 cells. The crosstalk between murine M34 MΦs and Th1/Th17 cells broadens the inflammatory and metabolic phenotypes resulting in the expansion of IL-34 pathogenicity. Consequently, IL-34-instigated joint inflammation was alleviated in RAG-/- compared to wild type mice. Consistently, SDC-1 deficiency attenuated IL-34-induced arthritis by interfering with joint glycolytic M34 MΦ and osteoclast remodeling. Similarly, inhibition of glycolysis by 2-DG reversed the joint swelling and metabolic rewiring triggered by IL-34 via HIF1α and C-MYC induction.

Conclusion: IL-34 is a novel endogenous factor that remodels hypermetabolic M34 MΦs and facilitates their cross-regulation with effector T cells to advance RA inflammatory bone destruction.

Rheumatoid arthritis (RA) is an autoimmune disorder characterized by an abundance of inflammatory cytokines, propagating immune cell infiltration, painful joint swelling and late-stage cartilage and bone erosion (1). Macrophages (MΦs) substantially contribute to this cytokine-rich inflammatory milieu (2). Independent of the underlying cause of RA, activated MΦs are highly involved in pannus remodeling and radiological progression (3, 4). RA standard-of-care therapies primarily target TNFα and IL-6 function, however, up to 50% of patients either don't respond or lose their responsiveness to these therapies over-time.

Earlier studies have shown that RA naïve $CD4^+$ T cells undergo a distinct metabolic reconfiguration, shifting from glucose metabolism to the pentose phosphate pathway, which supports a biased Th1/Th17 polarization (5, 6). RA fibroblasts activated with PDGF or TNFα can increase glucose metabolism via glycolysis and oxidative phosphorylation (7-9). Studies in cancer, atherosclerosis and obesity have revealed that polarization of M1 MΦs promotes metabolic reprogramming towards glycolysis and away from oxidative phosphorylation (10, 11). Recent reports elucidated that hypermetabolic ATP^{high} ROS^{high} MΦs are characterized by hyperglycolysis which is linked to the expansion of glucose transporters and glycolytic enzymes (12, 13). Yet, the endogenous factors and the mechanism by which RA MΦs are reprogrammed remain unclear.

Recently, Interleukin-34 (IL-34) has gained interest as a novel biomarker for RA (14). Serum levels of IL-34 correlate with several RA markers, including C-reactive protein (CRP),

erythrocyte sedimentation rate (ESR), rheumatoid factor (RF) and anti-cyclic citrullinated peptide (CCP) antibody (Ab) (15). A correlation was also found between synovial IL-34 expression and the accumulation of leukocytes in RA synovial fluid (SF) (14). Additionally, IL-34 expression and function have been implicated in other diseases, such as breast and lung cancer, liver fibrosis, type 2 diabetes and cardiovascular dysfunction (16, 17). IL-34's mechanism of action has predominately been attributed to M-CSFR, a receptor shared with macrophage colony-stimulating factor (M-CSF). M-CSF binding to M-CSFR cultivates immunosuppressive M2 MΦs (18, 19). In contrast, the impact of IL-34 on the MΦ profile remains unresolved. Conflicting reports support either an inflammatory (20) or an immunosuppressive (21, 22) phenotype for IL-34-differentiated MΦs. This controversy carries over to the indirect effect of IL-34 on T effector cell polarization. IL-34 has been reported to stimulate Th17 cell polarization, via IL-1α and IL-6, thereby aggravating autoimmune RA pathogenesis (15, 20, 23). In contrast, others demonstrated that the immunoregulatory MΦs polarized by IL-34 promote transplant tolerance by expanding the FOXP3^{+} Treg population (24).

Interestingly, Syndecan-1 (SDC-1), a heparin sulfate proteoglycan that functions as a co-receptor to M-CSFR, modulates IL-34's biological activity (25). Since M-CSF does not bind to SDC-1, its involvement could account for a distinct pathway that is unique to IL-34-mediated pathology. Although an extensive number of studies have shown that SDC-1 potentiates tumorigenesis by regulating cancer cell invasion, survival and metastasis (26, 27), its pathogenic role is undetermined in RA.

We investigated the arthritogenic potential of IL-34 and SDC-1 and their impact on RA immunometabolism. It was observed that in RA MΦs, SDC-1 triggers M-CSFR phosphorylation upon IL-34 binding. IL-34 rewired naïve cells into glycolytic CD14^{+}CD86^{+}GLUT1^{+} M34 MΦs which were disrupted by M-CSFR or SDC-1 blockade. In SDC-1-/- and RAG-/- mice, dysregulation of M34 MΦ reprogramming and their deficient crosstalk with Th1/Th17 cells reversed IL-34-elicited joint inflammation and osteoclast formation. Furthermore, 2-DG therapy substantiated that M34 MΦ metabolic remodeling via HIF1α and C-MYC may be indispensable for IL-34-induced arthritis. In short, restricting the function of IL-34 or its co-receptors may provide a promising therapeutic strategy for RA patients.

MATERIALS AND METHODS

Patient samples

Peripheral blood (PB) and synovial fluid (SF) samples were collected according to our protocol approved by the University of Illinois at Chicago Institutional Ethics Review Board. Normal (NL) subjects, osteoarthritis (OA) and RA patients participated in this study, after providing informed consent. RA patients were diagnosed according to the 1987 revised criteria of ACR (28). Human PB mononuclear cells (PBMCs) were isolated by density gradient centrifugation using Ficoll-Paque Premium. Monocytes were negatively selected using the EasySep human monocyte enrichment kit (StemCell Technologies) according to the manufacturer's instructions. Monocytes were cultured in 20% FBS/RPMI for 2-3 days to obtain *in vitro* differentiated naïve MΦs. RA FLS were isolated from digested (Dispase/Collagenase/DNase) fresh RA ST as previously described (29, 30). More detail about the study design, methods and the antibodies used for flow cytometry, IHC and WB are provided in the Supplementary material.

Western blot

Cell lysates from *in vitro* differentiated MΦs, peripheral blood T cells, or RA FLS were probed for SDC-1 and M-CSFR to validate receptor expression. Actin was detected to confirm equal loading. Blots were probed for phosphorylated signaling molecules or the activated phosphorylated M-CSFR (Y723) compared to either Actin or GAPDH.

Flow cytometry

Negatively selected monocytes were differentiated *in vitro* and stimulated with IL-34 (300 ng/ml) or untreated (Ctrl) for 24h before staining with CD14-FITC, CD86-APC and CD206-PECy7 Abs or DAPI. Viable (DAPI-negative) cells were analyzed for double-positive CD14$^+$CD86$^+$, CD14$^+$CD206$^+$, CD14$^+$GLUT1$^+$ populations. Untreated, viable (DAPI negative) RA FLS were stained to determine baseline PTPRZ1 surface expression with PTPRZ1-PE Ab. The concentration of Abs is indicated in supplementary table 1. The supplementary figure S6 exemplifies the used gating strategy.

Seahorse cell energy phenotype test

The glycolytic capacity (ECAR) or oxygen consumption (OCR) was evaluated in RAW 264.7 cells (5×10^3 cells/well) in response to control (PBS) or IL-34 treatment using the Cell Energy Phenotype Test kit (Agilent Technologies) as per the manufacturer's instructions. Cells were pre-conditioned with the stimuli for in 0% FBS/DMEM, for 24h before ECAR and OCR assessment.

Osteoclastogenesis assay

Osteoclastogenesis was evaluated following the previously described protocol (31). BM-derived myeloid precursors (4 days of M-CSF) cultured in 10% FBS/αMEM were either untreated (Ctrl) or conditioned with suboptimal levels of RANKL/M-CSF (both 15 ng/ml; 15/15), with or without IL-34 (300 ng/ml). Stimulation media was refreshed 2x/week for 2 weeks and TRAP+ osteoclasts were stained (387A-1KT; Sigma-Aldrich).

Animals

All animal studies were approved by the UIC Animal Care and Use Committee. WT and RAG1-/- (RAG-/-) C57BL/6 mice were purchased from Jackson Laboratory. SDC-1-/- mice were generated as previously described (26) and kindly provided by Dr. Caroline Alexander (University of Wisconsin-Madison). Mice (≥8 weeks old) were injected i.a. with adenovirus (Ad)-Ctrl or Ad-IL-34 (3×10^{10} VP/ankle), on days 0, 7 & 14. Mice treated with 2-DG were injected i.p. at 7.5 mg/kg BW on days 0, 3, 7, 9, 11, 14 & 15. Mice were sacrificed on different days as specified in figure legends.

Immunohistochemistry

Human formalin-fixed paraffin-embedded tissue samples were sectioned. NL, OA and RA STs were stained to quantify IL-34, M-CSFR, SDC-1 and PTPRZ1 presentation. Staining was scored blinded, distinguishing staining within the synovial lining, sublining and vasculature (0-5 scale) (29, 32). Formalin-fixed mouse ankles were decalcified and paraffin-embedded. Slides were deparaffinized in xylene and antigen retrieval was achieved as previously described (33). Mouse ankle sections were stained for MΦ (F4/80, iNOS, Arg1), T cell (CD3) and fibroblast (Vimentin) markers, or for transcription factors C-MYC and HIF1α. The

supplementary table S1 specifies the Abs used and their dilutions. The stained joint tissues were scored for inflammation, synovial lining thickness and bone erosion on a 0-5 scale (29, 32).

Statistical Analysis

GraphPad Prism 8 software was used to generate figures and to perform statistical analysis. Bar graphs present mean values ± SEM. Box-and-whisker plots visualize data distribution, from minimum to maximum with a centerline that defines the median. Where appropriate, individual datapoints were shown. ANOVA was first used to verify statistical significance when comparing multiple groups. Differences between the two groups were evaluated by a two-tailed unpaired t-test unless otherwise specified in the figure legends.

RESULTS

IL-34, SDC-1 and M-CSFR are highly expressed in RA synovium

Studies were conducted to characterize the expression and functional significance of IL-34 and its receptors in RA. Levels of IL-34, M-CSF and Granulocyte-Macrophage Colony-Stimulating Factor (GM-CSF) were quantified, in the plasma of NL, OA and RA, as well as in the SF of OA and RA. Although IL-34 levels were comparable among all plasmas, its concentration was significantly higher in RA compared to OA SF (12x), unlike M-CSF and GM-CSF (Fig. 1A). Histological studies substantiate the elevated expression of IL-34 in RA compared to OA and NL synovial tissues (STs) lining and sublining (Fig. 1B, suppl-Fig. S1A). However, M-CSFR expression was similar in all STs lining and sublining, with a modest increase observed in RA and OA vasculature (Fig. 1C, suppl-Fig. S1B). While M-CSFR is the primary receptor for IL-34, a co-receptor that modulates IL-34/M-CSFR signaling has been identified. We confirmed that IL-34 binds to the proteoglycan SDC-1 (2.5 μg) with a half-maximal effective concentration (EC$_{50}$) of 3 ng/ml (Fig. 1D). Histological analysis revealed that the SDC-1 presentation was expanded in RA compared to OA and NL ST lining and sublining (Fig. 1E, suppl-Fig. S1C). The endothelial distribution of SDC-1 was similarly amplified in RA and OA ST compared to NL ST. Next, the expression of IL-34's receptors was evaluated in RA MΦs, T cells and fibroblast-like synoviocytes (FLS) (Fig. 1F). Unlike SDC-1 that is expressed on RA MΦs, T cells and RA FLS, M-CSFR expression is restricted to RA MΦs as its extra- & intracellular domains are only present on these cells (140 & 52 kDa). Fluorescence microscopy

confirmed that IL-34 and its receptors, M-CSFR and SDC-1, co-localize in RA ST particularly in the lining layer (suppl-Fig. S1D). These results indicate that IL-34 levels are highly potentiated in RA SF and ST; and MΦs by expressing the SDC-1/M-CSFR receptor complex are the main effector cells that control IL-34 activity.

Local IL-34 expression triggers immune cell extravasation and joint inflammation

Next, experiments were performed to evaluate the arthritogenic potential of IL-34. Intra-articular administration of IL-34 triggered progressive joint inflammation (Fig. 2A), along with exacerbated lining thickness and immune cell infiltration (Figs. 2B, suppl-Fig. S2A). Histological analysis revealed that IL-34-induced joint inflammation was accompanied by the accumulation of F4/80[+] MΦs, predominately characterized as inflammatory iNOS^{+} cells (Fig. 2C, suppl-Fig. S2B). In contrast, the number of F4/80[+]Arginase1[+] MΦs was unchanged in IL-34 arthritic mice relative to the control group. Consistently, expression of monokines such as CCL5 (302x), IL-1β (36x), TNFα (27x), CCL2 (24x), CXCL2 (20x), and IL-12 (4x) was amplified in IL-34 arthritic mice compared to the control group (Figs. 2D-E). In IL-34 arthritic mice, the transcriptome data were validated by the increased joint CCL5, IL-1β, CCL2, and IL-6 protein levels (12x up to 1407x vs control) (suppl-Figs. S2C-F). Except for Receptor Activator of NFκ-B ligand (RANKL), transcription of the osteoclastogenic markers, RANK, Nuclear Factor Of Activated T-Cells c (NFATc), Cathepsin K (CTSK) and TRAP, was upregulated by 15-, 3-, 7- and 12-fold respectively, in IL-34 arthritic joints compared to their control counterparts (Fig. 2F). Taken together, local IL-34 provokes arthritis, characterized by inflammatory F4/80[+]iNOS[+] MΦs and RANK[high] osteoclasts.

IL-34 remodels monocytes into inflammatory M34 MΦs in an SDC-1-dependent manner

Expression of IL-34 and its co-receptors in RA MΦs, as well as the amplified transcription of monokines in IL-34 arthritic mice, implied that MΦs are both producers and responders of IL-34. To delineate the mechanism of IL-34, in connection with SDC-1, we examined the activation of M-CSFR and its downstream pathways. IL-34 binding triggered M-CSFR phosphorylation (tyrosine Y723), which was accompanied by the activation of ERK and p38 MAPK pathways (suppl-Figs. S2I-J). In RA MΦs, SDC-1 Ab pretreatment markedly

reduced M-CSFR (tyrosine Y723) and ERK phosphorylation triggered by IL-34 stimulation (Figs. 3A, quantified in suppl- Figs. S2G-H). This suggests that SDC-1 controls the initial M-CSFR activation and its downstream signaling pathways.

Naïve progenitor cells stimulated with IL-34 exhibited a significant increase in CD14$^+$CD86$^+$ MΦs frequency (Fig. 3B, suppl-Fig. S3A). Consistently, while the MFI for CD14$^+$CD206$^+$ MΦs remained unchanged, IL-34 activation expanded the MFI for CD14$^+$CD86$^+$ MΦs (suppl-Fig. S3A). Reprogramming of M0 cells into M34 MΦs by IL-34 transformed their cytokine profile. In M34 MΦs, transcription of IL-1β, CXCL8 and CCL2 (3-4x) was upregulated, whereas IL-10 expression was diminished and TGFβ levels were unaffected (Fig. 3C, suppl-Fig. S3B). Moreover, we substantiated that RA M34 MΦs secrete higher levels of CXCL8, CCL2, TNFα and IL-6 (suppl-Fig. S3C). Nevertheless, this distinct profile of M34 MΦs was disrupted by M-CSFR or SDC-1 Abs, as displayed by the downregulated TNFα, IL-6 and CCL2 production (upregulation reduced by 105, 91 and 58%, respectively) (Figs. 3D-F). In conclusion, the blockade of M-CSFR and SDC-1 function reversed the RA M34 MΦ inflammatory profile.

Subsequently, we asked if IL-34 could influence other myeloid cell functions such as phagocytosis. We found that in RA MΦs, IL-34 interferes with zymosan-triggered phagocytosis similar to the established inhibitor Cytochalasin D (suppl-Fig. S3D). These results indicate that IL-34 advances the inflammatory phenotype in RA MΦs by disrupting phagocytosis.

IL-34 reprograms naïve myeloid cells into glycolytic M34 MΦs

RA MΦ reprogramming, instigated by IL-34, expands the population of CD14$^+$GLUT1$^+$ cells (Figs. 4A, suppl-Fig. S3E). Also in murine MΦs, the extracellular acidification rate (ECAR; reflects glycolysis) was dose-dependently accentuated by IL-34 for the entire study duration (0 to 55 min)(Fig. 4B). In contrast, only a brief, transient escalation of the oxygen consumption rate (OCR; reflects oxidative phosphorylation) was noted in IL-34 activated murine MΦs following FCCP treatment which maximizes the oxidative potential (suppl-Fig. S3F). In line with their increased glycolytic metabolism, IL-34-differentiated BM-derived MΦs produced higher levels of L-lactate and pyruvate (Fig. 4C). These murine M34 MΦs exhibited a skewed profile, which favored the glycolytic factors over the pentose phosphate pathway (PPP) or oxidative regulators

which resulted in CARKL or PPARγ reduction (Fig. 4D). Accordingly, compared to non-arthritic mice, IL-34 arthritic joints displayed a significant upregulation in master modulators of glycolysis, GLUT1 (2x), PFKFB3 (2x), as well as glycolytic transcription factors, C-MYC (3x) and HIF1α (4x) (suppl-Fig. S3G). Since M34 MΦ polarization was linked to increased GLUT1 and glucose uptake, blood glucose concentration was downregulated following 15 min and 30 min of glucose injection in arthritic compared to control mice (suppl-Fig. S3H).

Intriguingly, we reveal that i.p. injection of 2-Deoxy-D-glucose (2-DG), an inhibitor of glycolysis, alleviates IL-34-induced joint swelling (Fig. 4E). Morphological studies substantiate that C-MYC and HIF1α expression, as well as F4/80$^+$iNOS$^+$ MΦs and CD3$^+$ T cell infiltration, was curtailed in IL-34 arthritic mice that received 2-DG therapy compared to those in the placebo group (Fig. 4F, suppl-Figs. S3J-L). Joint lining thickness and inflammation were similarly reversed by 2-DG treatment (Fig. 4F, suppl-Fig. S3I). Collectively, we demonstrate for the first time that IL-34 is an endogenous factor that can reprogram RA MΦ metabolic activity.

IL-34 induces RA FLS migration, independently of SDC-1 and M-CSFR

In vivo, ectopic IL-34 expression expanded joint Vimentin$^+$ fibroblast infiltration (suppl-Fig. S4A). *In vitro*, IL-34 did not significantly activate any of the evaluated signaling pathways in RA FLS, although a trend was observed for p38 phosphorylation (suppl-Fig. S4B). As previously established, RA FLS abundantly expresses SDC-1 (Fig. 1F). Despite the lack of full-length M-CSFR in RA FLS, IL-34 markedly activated FLS migration compared to the control treatment (suppl-Fig. S4C). Surprisingly, blockade of SDC-1 or M-CSFR function was incapable of preventing IL-34-induced RA FLS migration. Since IL-34 has also been reported to induce M-CSFR-independent signaling through PTPRZ1, we examined the role of this proteoglycan. IL-34-mediated RA FLS migration was reduced by anti-PTPRZ1 Ab treatment (suppl-Fig. S4D), despite the rather modest expression of PTPRZ1 on RA FLS (suppl-Fig. S4E; 6% PTPRZ1$^+$ RA FLS). Unlike SDC-1, PTPRZ1 expression was not elevated in RA nor OA ST compared to NL ST (suppl-Fig. S4F). Due to the missing connection between PTPRZ1 and RA pathogenesis, this IL-34 study was focused on SDC-1 and its modulation of IL-34/M-CSFR activity. In short, we found that IL-34 triggers joint as well as RA FLS recruitment independent of its primary co-receptors.

RA FLS inflammatory response and immunometabolism were not modulated by IL-34

IL-34 reprograms SDC-1$^+$M-CSFR$^+$ MΦs into glycolytic and inflammatory M34 MΦs, while transcription and/or translation of IL-6, CXCL8, CCL2 and CCL5 were unaffected by IL-34 in RA FLS (suppl-Fig. S4G-H). Corroborating these data, transcriptional regulation of GLUT1, HK2, PFKFB3, PKM2, LDHA, C-MYC and HIF1α was unchanged by IL-34 stimulation (suppl-Fig. S4I). Taken together, these results support that the SDC-1/M-CSFR complex is indispensable for the inflammatory and hyperglycolytic effects of IL-34, as seen in RA MΦs.

T effector cells contribute to IL-34-induced arthritis

IL-34 promotes Th17 cell polarization of SDC-1$^+$M-CSFR$^-$ CD4$^+$ T cells in an indirect manner (15, 20, 23). We found that IL-34-induced Th17 cell differentiation of murine splenocytes co-cultured with BMMΦs requires glycolytic cell metabolism, as 2-DG treatment diminished this process (Fig. 5A). In addition to MΦs, CD3$^+$ T cell infiltration was potentiated in IL-34 arthritic ankle joints (Figs. 5B, suppl-Fig. S5A). Furthermore, IL-34 amplified joint Th1/Th17 cell polarization, as reflected by the exacerbated IFNγ and IL-17 production (suppl-Figs. S5B-C). To validate the involvement of T cells in IL-34-induced arthritis, RAG-/- mice received i.a. IL-34 injection. IL-34-induced joint swelling was mitigated in RAG-/- compared to wild type (WT) mice starting on day 9 and throughout the study (Fig. 5C). Morphological studies displayed that the synovial lining was similarly aggravated by local IL-34 expression in RAG-/- and WT mice (Fig. 5D, suppl-Fig. S5D). The number of joint F4/80$^+$iNOS$^+$ MΦs was not disrupted in RAG-/- compared to WT mice that received local IL-34 administration (Fig. 5D, suppl-Fig. S5E). Despite this, expansion of joint IL-1β, CCL5, CXCL2 and TGFβ levels (but not TNFα and CCL2) in the IL-34 arthritic animals, were reduced in RAG-/- compared to WT mice (Fig. 5E).

Nonetheless, IL-34-induced bone erosion was downregulated in RAG-/- relative to WT mice, in part due to the absence of T cell-produced RANKL (Fig. 5F). Loss of RANKL function in RAG-/- mice interferes with IL-34-induced upregulation of NFATc and TRAP but not CTSK (Fig. 5F). Overall, IL-34-induced arthritis is exacerbated by T cell involvement, yet MΦs initiate and shape the signature IL-34-driven arthritic phenotype.

SDC-1 defines the IL-34-induced immunostimulatory phenotype

To solidify the importance of SDC-1 as a central modulator of IL-34-mediated disease, genetically modified mice lacking SDC-1 were utilized (26). Progression of IL-34-induced arthritis was severely reduced in SDC-1-/- mice throughout the study (Fig. 6A). Notably, in the absence of SDC-1, local expression of IL-34 did provoke minor joint swelling, perhaps due to marginal M-CSFR activation. In IL-34 arthritic mice, upregulation of joint IL-1β, CCL2, CXCL2 and CCL5 but not TNFα was impaired in SDC-1-/- compared to the WT mice (reduced by 81, 66, 84 and 57%, respectively; Fig. 6B, suppl-Fig. S5F).

In murine BM-derived MΦs, transcription of several components of the glycolytic pathway, including GLUT1, HK2, LDHA, C-MYC and HIF1α, was amplified by IL-34 stimulation (Fig. 6C). Although expression of HK2 and C-MYC was suppressed, levels of GLUT1, LDHA and HIF1α remained unchanged in IL-34 activated SDC-1-/- progenitor cells relative to the control group (Fig. 6C). Altogether, we conclude that IL-34's interaction with SDC-1 shifts naïve cells to glycolytic M34 MΦs that have a unique inflammatory and metabolic phenotype.

SDC-1 is indispensable for osteoclasts differentiated by IL-34

In IL-34-induced arthritis, we demonstrated that the formation of TRAP+ osteoclasts was in part due to increased RANK expression, which was disrupted in SDC-1-/- mice (Fig. 6D). TRAP staining corroborated that IL-34-induced osteoclast formation was compromised in SDC-1-/- progenitor cells compared to WT mice (Figs. 6E, suppl-Fig. S5G). Taken together, our data indicate that SDC-1+ MΦs in conjunction with T cells advance IL-34-modulated osteoclastogenesis in part through RANK/RANKL function.

DISCUSSION

The current study describes a novel role for IL-34 and its co-receptor SDC-1 in RA pathogenesis. We showed that SDC-1 regulates myeloid IL-34/M-CSFR signaling and downstream functions. Activation of the receptor complex SDC-1/M-CSFR is essential for the reconfiguration of naïve cells to glycolytic and inflammatory CD14+CD86+GLUT1high M34 MΦs. Arthritic IL-34-differentiated F4/80+iNOS+ MΦs are characterized by the transcriptional upregulation of glycolytic mediators, HIF1α and C-MYC, which are dysregulated by systemic 2-

DG therapy. Intriguingly, SDC-1 or T cell deficiency counteracts IL-34-induced joint inflammation and osteoclastic erosion in part by interfering with the hyperglycolytic activity (Fig. 6F).

The higher bioavailability of IL-34 compared to M-CSF in the RA SF emphasizes its ability to outcompete M-CSF for M-CSFR binding. In contrast to the shared receptor M-CSFR, the co-receptor SDC-1, which does not bind M-CSF, is highly upregulated in RA ST lining and sublining. Joint GM-CSF levels are also less abundant than IL-34, and it does not compete for M-CSFR or SDC-1 binding. A growing body of evidence demonstrated that the IL-34 is involved in various pathologies, particularly in arthritis (14, 34). We showed that in RA MΦs, phosphorylation of M-CSFR by IL-34 is dependent on SDC-1. Others have shown that SDC-1 Ab impairs IL-34-mediated monocyte migration (35). SDC-1 manipulates the binding affinity of IL-34 to M-CSFR (27); hence remodeling joint MΦs to glycolytic and osteoclastic phenotypes.

SDC-1 expression is potentiated in a range of inflammatory as well as malignant disorders (36). In cancer, elevated SDC-1 levels are linked to exacerbated tumor size and poor prognosis. SDC-1 is involved in tumor invasion, proliferation, apoptosis and angiogenesis (37). Thus, inhibitory SDC-1 peptides and anti-SDC-1 Ab have been generated for immunotherapy of different cancers (38). In agreement with its pathogenic implications, we show that SDC-1 expression was highly upregulated in RA compared to NL ST lining and sublining, attributed to MΦs, T cells and RA FLS. Similar to RA joints, SDC-1 is highly expressed on PsA STs mononuclear infiltrates, while barely detectable in OA ST (39). In contrast, others have suggested that SDC-1 is involved in early-stage cartilage degeneration in experimental OA (40). It has also been shown that cannabinoid therapy attenuates OA disease activity by suppressing SDC-1 expression (41). Nevertheless, we demonstrated that SDC-1 upregulation in OA relative to NL STs was restricted to the vasculature. A limitation identified in this study was due to RA STs being collected from de-identified patients, and therefore the expression levels of IL-34, M-CSFR, and SDC-1 could not be linked to clinical parameters.

Our data underline that IL-34-differentiated MΦs diverge from M-CSF-induced M2 or GM-CSF-derived M1 MΦs (42). The pathogenic M34 MΦs don't rely as heavily on IL-6 or TNFα, both of which are successfully targeted by the current RA biologic therapies. Additionally, M34 MΦs displayed a glycolytic profile akin to that of hypermetabolic RA MΦs,

yet deviating from the metabolic signature reported in LPS-induced M1 MΦs. IL-34 potentiates the expression of two central glycolytic transcription factors, C-MYC and HIF1α, resembling RA MΦs (43-45). However, LPS has been shown to upregulate HIF1α exclusively, while suppressing C-MYC transcription (46). In IL-34 arthritic mice, 2-DG therapy interfered with C-MYC and HIF1α amplification and joint swelling, highlighting that the glycolytic rewiring is linked to the IL-34-modulated inflammatory phenotype. Intriguingly, both C-MYC and HIF1α have also been shown to instigate osteoclast formation (47). In addition to metabolic activity, RANK[high] M34 osteoclast progenitor cells are exceptionally sensitive to T cell-derived RANKL and are prone to undergo osteoclastogenesis.

In MΦs, M-CSF, unlike GM-CSF, favors mitochondrial oxygen consumption over glycolysis, as determined by the OCR/ECAR ratio (48). IL-34 has been suggested to induce M2 MΦ differentiation and enhance mitochondrial oxidative phosphorylation via the AMPK pathway (21). In contrast, our findings identify IL-34 as a glycolytic stimulus, as evidenced by prolonged ECAR/OCR activity, accentuated pyruvate and L-lactate secretion and transcriptional upregulation of metabolic intermediates in MΦs. Intriguingly, IL-34-driven metabolic reprogramming is expanded beyond MΦs, since 2-DG treatment negates IL-34-instigated Th17 cell polarization, suggesting that hypermetabolic activity is responsible for M34 MΦ cross-regulation with Th17 cells.

We noted that a wider range of cytokines was expressed in IL-34 arthritic mice, compared to RA MΦs differentiated by IL-34. Perhaps, Th1/Th17 cell differentiation in IL-34 arthritic mice exacerbates M34 MΦ immunometabolism. Extending these findings, joint inflammation and bone erosion advanced by local IL-34 were ameliorated in T cell-deficient RAG-/- compared to WT mice due to impaired joint IL-1β, CCL5, CXCL2, and NFATc expression. In SDC-1-/- mice, IL-34-induced joint inflammation was alleviated through a similar mechanism as RAG-/- mice (IL-1β, CCL5, CXCL2); nevertheless, osteoclastogenesis was restrained via RANK reduction. Hence, the crosstalk between the metabolic T effector cells and M34 pre-osteoclasts plays a critical role in IL-34-elicited inflammatory erosion. In agreement with these observations, earlier studies have illustrated that IL-34 is responsible for Th17 cell differentiation (15, 20, 23). Controversially, others have reported that IL-34-stimulated MΦs promote CD4^{+}FOXP3^{+} Treg differentiation and thereby facilitate allograft tolerance (24).

Although TNFα and PDGF promote hypermetabolic activity in RA FLS (9), neither their immunometabolic nor inflammatory profile is altered by IL-34 stimulation. Opposing our findings, IL-6 and CXCL8 were secreted from lung fibroblasts in response to IL-34 stimulation (49). Interestingly, while IL-34 advances RA FLS migration, this function is disconnected from the inflammatory or glycolytic activity in these cells. Hence, the inability of SDC-1 or M-CSFR blockade to negate IL-34-triggered motility suggested that RA FLS trafficking was fostered by an alternative pathway. Remarkably, IL-34 can function independent of M-CSFR or SDC-1, through a different heparin sulfate proteoglycan, namely PTPRZ1 (50). Modest levels of PTPRZ1 in RA FLS were shown to be responsible, at least in part, for the IL-34-mediated infiltration. However, unlike SDC-1, PTPRZ1 is similarly expressed in RA compared to OA and NL STs. This is a departure from the magnified expression of PTPRZ1 on glioblastoma and colorectal cancer cells and its implication in advancing other IL-34-mediated pathologies (50, 51).

Collectively, we have shown for the first time that hyperglycolytic M34 MΦs and effector Th17 cells participate in inflammatory and erosive phenotypes enforced by joint IL-34 expression. While our preclinical data are promising, the therapeutic potential of IL-34 and its downstream metabolic intermediates remain to be elucidated.

FIGURE LEGENDS

Figure 1. Expression of IL-34 and its receptors, M-CSFR and SDC-1, in NL, OA and RA specimens. (**A**) GM-CSF, M-CSF and IL-34 protein concentrations were determined in plasma and SF samples collected from NL (plasma: n=39), OA (plasma: n=10; SF: n=32) and RA (plasma: n=39; SF: n=45) donors. NL, OA and RA synovial tissues were stained for IL-34 (**B**), M-CSFR (**C**) and SDC-1 (**E**) and scored on a 0-5 scale in suppl-Fig. S1A-C (for IL-34, NL: n=9, OA: n=11, RA: n=9; for M-CSFR, NL: n=9, OA: n=11, RA: n=8; for SDC-1, NL: n=8, OA: n=10, RA: n=10). (**D**) A biotinylated anti-IL-34 Ab was used to compare the amount of IL-34

retained on a recombinant SDC-1-coated plate versus a PBS-coated plate, both incubated with various doses of IL-34 (0.24 to 1000 ng/ml). **F**) Western blot analysis was used to evaluate the expression of SDC-1 (32 kDa) and M-CSFR (full-length: 140 kDa; intracellular domain: 52 kDa) in RA PB MΦ, T cells and RA FLS. Equal loading was confirmed by quantifying Actin (42 kDa). The data are shown as mean ± SEM. * $p<0.05$ ** $p<0.01$ *** $p<0.001$.

Figure 2. Joint inflammation was induced by local IL-34 expression. WT mice were i.a. injected 1x/week with Ad-Ctrl and Ad-IL-34. (**A**) Joint circumference was monitored over 16 days (n=16). 16 days post-onset, mice were sacrificed and joints were processed for IHC, qRT-PCR and protein estimation. (**B**) Tissue sections were stained with H&E and scored for synovial lining thickness, inflammation and bone erosion on a 0-5 scale in the suppl-Fig. S2A (n=5). (**C**) Tissue sections were stained for MΦ markers F4/80, iNOS, Arg1 and staining was scored on a 0-5 scale in the suppl-Fig. S2B (n=5). By qRT-PCR, joint RNA levels of various monokines (**D-E**) or osteoclastic factors (**F**) were determined following Ad-IL-34 or control treatment (n=8). The data are shown as mean ± SEM or as minimum-maximum box-and-whisker plots (centerline = median). * $p<0.05$ ** $p<0.01$ *** $p<0.001$.

Figure 3. M34 MΦ signaling and signature is dependent on SDC-1 ligation. (**A**) Cells were pre-incubated with buffer, anti-SDC-1 Ab (1:100) or anti-M-CSFR Ab (10 µg/ml) for 2h before IL-34 (100 ng/ml) stimulation for 5 or 10 minutes and lysates were used for WB quantification of pM-CSFR and pERK. WB shown is one representative out of 4 independent experiments. (**B**) *In vitro* differentiated MΦs derived from negatively selected RA monocytes were control-treated or stimulated with IL-34 (300 ng/ml) for 24h and then stained with Ab against CD14, CD86 and CD206 for flow cytometry. (**B**) The contour plot of CD14$^+$ CD86$^+$ cells for one representative experiment out of 5 is shown. Among CD14$^+$ gated cells, the MFI of CD86 and CD206 staining was determined (n=5) in the suppl-Fig. S3A. (**C**) The qRT-PCR analysis was performed to determine the expression of M1 and M2 cytokines by RA *in vitro* differentiated MΦs stimulated with IL-34 (300 ng/ml) for 8h, expressed as a fold change compared to control treatment (n=4). (**D-F**) Prior to IL-34 stimulation, RA cells were control-treated or pre-incubated with anti-SDC-1 (1:100) or anti-M-CSFR Ab (10 µg/ml) (CCL2: n=8; TNF: n=6; IL-6: n=8). Protein induction was compared to control treatment and was analyzed using the Wilcoxon signed-rank test. The effect of neutralizing Abs compared to sole IL-34 stimulation was analyzed using a one-tailed

Wilcoxon matched-pairs signed-rank test. The data are shown as mean ± SEM or as minimum-maximum box-and-whisker plots (centerline = median). * p<0.05 ** p<0.01 *** p<0.001.

Figure 4. IL-34-induced metabolic changes promote progressive inflammation. (**A**) *In vitro* differentiated MΦs, derived from negatively selected monocytes, were control-treated or stimulated with IL-34 (300 ng/ml) for 24h. A representative contour plot and the mean percentage of CD14$^+$GLUT1$^+$ cells (n=5) are shown. Significance was evaluated using a paired t-test. (**B**) The Seahorse cell energy phenotype assay was employed to study the glycolytic (ECAR) capacity of PBS- *versus* IL-34-pre-treated RAW 264.7 cells (n=5). (**C**) The concentration of L-lactate and pyruvate in the conditioned media of murine MΦs (24h) was determined colorimetrically (n=4). (**D**) Under hypoglycemic conditions, murine BM-derived MΦs were untreated or stimulated with IL-34 (1 µg/ml) for 6h and expression of metabolic genes was examined by qRT-PCR (n=4). WT mice were i.a. injected 1x/week with Ad-Ctrl and Ad-IL-34. (**E**) The mice that received Ad-IL-34 were either i.p. treated with 2-DG or placebo and joint circumference was monitored over 16 days (n=10). (**F**) Tissue sections were stained for C-MYC and HIF1α or H&E stained and staining was scored on a 0-5 scale in the suppl-Figs. S3I-J (n=4). The data are shown as mean ± SEM or as minimum-maximum box-and-whisker plots (centerline = median). * p<0.05 ** p<0.01 *** p<0.001.

Figure 5. T cells contribute to IL-34-induced joint inflammation. (**A**) Supernatant levels of IL-17 were measured in the BMMΦ-splenocyte co-cultures (5 days) treated with control or IL-34 (1 µg/ml) in the presence or absence of 2-DG (5 mM) (n=3). As a positive control (+) co-cultures were stimulated with TGFβ (1ng/ml) + IL-6 (20 ng/ml). (**B**) Joint CD3+ T cells were stained in WT mice that received Ad-Ctrl and Ad-IL-34 on days 0, 7, 14, and were sacrificed on day 16. Immunostaining was scored on a 0-5 scale in the suppl-Fig. S5A (n=5). (**C**) Joint circumference was monitored in WT and RAG-/- mice that were i.a. injected with Ad-Ctrl or Ad-IL-34 (1x/week) and were sacrificed on day 17 (n=10). (**D**) Ankle joints were stained for H&E or F4/80, iNOS and Arg1 (n=4). H&E and positive MΦ immunostaining were scored on 0-5 scale in the suppl-Fig. S5D-E. (**E**) Joint expression of monokines (Ad-Ctrl (WT): n=7; Ad-IL-34 (WT): n=5; Ad-IL-34 (RAG-/-): n=6) and osteoclastic factors (**F**; n=6) were determined by qRT-PCR. The data are shown as mean ± SEM. * p<0.05 ** p<0.01 *** p<0.001.

Figure 6. SDC-1 modulates IL-34-driven joint inflammation, glycolysis and osteoclastogenesis. WT and SDC-1-/- mice were i.a. injected with Ad-Ctrl or Ad-IL-34 (1x/week). (**A**) Joint circumference was monitored over 15 days, thereafter mice were sacrificed and differences between treatment groups were evaluated using the non-parametric Mann-Whitney test (Ad-Ctrl (WT): n=7; other groups: n=8). (**B**) Transcriptional regulation of joint inflammatory mediators was evaluated by qRT-PCR (n=4). (**C**) Under hypoglycemic conditions, BMMΦs from WT and SDC-1-/- mice were untreated or stimulated with IL-34 (1 µg/ml) for 6h and expression of glycolytic genes was examined by qRT-PCR (n=4). (**D**) Transcription levels of joint osteoclastic factors were determined by qRT-PCR in WT and SDC-1-/- mice that received control or Ad-IL-34 local injection (n=4). (**E**) To assess osteoclastogenesis *in vitro*, BM-derived pre-osteoclasts from WT and SDC-1-/- mice were untreated (-Ctrl), cultured in suboptimal conditions (15 ng/ml M-CSF and RANKL; 15/15) or exposed to 15/15 + IL-34 (300 ng/ml). Following 14 days of differentiation (fresh stimuli 2x/week), TRAP staining was performed and TRAP⁺ multinuclear osteoclasts were counted in the suppl-Fig. S5G (n=4). (**F**) Illustrates that IL-34 binding to M-CSFR/SDC-1 cultivates RA inflammatory and glycolytic M34 MΦs that are predisposed to osteoclastogenesis. The data are shown as mean ± SEM, * p<0.05 ** p<0.01 *** p<0.001.

enable us to pursue clinically relevant translational research. We would also like to thank Mr. Brian Zanotti (Volin Lab, Midwestern University) for his technical assistance in performing the histological studies. We thank Prof. Alexander (University of Wisconsin-Madison) who kindly provided the SDC-1-/- mice used in this study.

COMPETING INTERESTS: Authors have no conflict of interest to report.

REFERENCES

1.   Brennan FM, McInnes IB. Evidence that cytokines play a role in rheumatoid arthritis. Journal of Clinical Investigation 2008;118:3537-45.

2.   McInnes IB, Buckley CD, Isaacs JD. Cytokines in rheumatoid arthritis - shaping the immunological landscape. Nature Reviews: Rheumatology 2016;12:63-8.

3.   McInnes IB, Schett G. The pathogenesis of rheumatoid arthritis. N Engl J Med 2011;365:2205-19.

4.   Mulherin D, Fitzgerald O, Bresnihan B. Synovial tissue macrophage populations and articular damage in rheumatoid arthritis. Arthritis Rheum 1996;39:115-24.

5.   Weyand CM, Goronzy JJ. Immunometabolism in early and late stages of rheumatoid arthritis. Nature Reviews: Rheumatology 2017;13:291-301.

6.   Yang Z, Shen Y, Oishi H, Matteson EL, Tian L, Goronzy JJ, et al. Restoring oxidant signaling suppresses proarthritogenic T cell effector functions in rheumatoid arthritis. Science Translational Medicine 2016;8:331ra38.

7.   Biniecka M, Canavan M, McGarry T, Gao W, McCormick J, Cregan S, et al. Dysregulated bioenergetics: a key regulator of joint inflammation. Annals of the Rheumatic Diseases 2016;75:2192-2200.

8.   Garcia-Carbonell R, Divakaruni AS, Lodi A, Vicente-Suarez I, Saha A, Cheroutre H, et al. Critical Role of Glucose Metabolism in Rheumatoid Arthritis Fibroblast-like Synoviocytes. Arthritis Rheumatol 2016;68:1614-26.

9.   Falconer J, Murphy AN, Young SP, Clark AR, Tiziani S, Guma M, et al. Review: Synovial Cell Metabolism and Chronic Inflammation in Rheumatoid Arthritis. Arthritis Rheumatol 2018;70:984-999.

10.   Geeraerts X, Bolli E, Fendt SM, Van Ginderachter JA. Macrophage Metabolism As Therapeutic Target for Cancer, Atherosclerosis, and Obesity. Frontiers in Immunology 2017;8:289.

11.   Viola A, Munari F, Sanchez-Rodriguez R, Scolaro T, Castegna A. The Metabolic Signature of Macrophage Responses. Frontiers in Immunology 2019;10:1462.

12.   Zeisbrich M, Yanes RE, Zhang H, Watanabe R, Li Y, Brosig L, et al. Hypermetabolic macrophages in rheumatoid arthritis and coronary artery disease due to glycogen synthase kinase 3b inactivation. Ann Rheum Dis 2018;77:1053-1062.

13.   Yoon BR, Oh YJ, Kang SW, Lee EB, Lee WW. Role of SLC7A5 in Metabolic Reprogramming of Human Monocyte/Macrophage Immune Responses. Front Immunol 2018;9:53.

14.   Chemel M, Le Goff B, Brion R, Cozic C, Berreur M, Amiaud J, et al. Interleukin 34 expression is associated with synovitis severity in rheumatoid arthritis patients. Ann Rheum Dis 2012;71:150-4.

15.   Wang B, Ma Z, Wang M, Sun X, Tang Y, Li M, et al. IL-34 Upregulated Th17 Production through Increased IL-6 Expression by Rheumatoid Fibroblast-Like Synoviocytes. Mediators of Inflammation 2017;2017:1567120.

16.   Rietkotter E, Bleckmann A, Bayerlova M, Menck K, Chuang HN, Wenske B, et al. Anti-CSF-1 treatment is effective to prevent carcinoma invasion induced by monocyte-derived cells but scarcely by microglia. Oncotarget 2015;6:15482-93.

17.   Ge Y, Huang M, Yao YM. Immunomodulation of Interleukin-34 and its Potential Significance as a Disease Biomarker and Therapeutic Target. Int J Biol Sci 2019;15:1835-1845.

18.   Hamilton TA, Zhao C, Pavicic PG, Jr., Datta S. Myeloid colony-stimulating factors as regulators of macrophage polarization. Front Immunol 2014;5:554.

19.   Huang SC, Smith AM, Everts B, Colonna M, Pearce EL, Schilling JD, et al. Metabolic Reprogramming Mediated by the mTORC2-IRF4 Signaling Axis Is Essential for Macrophage Alternative Activation. Immunity 2016;45:817-830.

20.   Foucher ED, Blanchard S, Preisser L, Descamps P, Ifrah N, Delneste Y, et al. IL-34- and M-CSF-induced macrophages switch memory T cells into Th17 cells via membrane IL-1alpha. European Journal of Immunology 2015;45:1092-102.

21.   Boulakirba S, Pfeifer A, Mhaidly R, Obba S, Goulard M, Schmitt T, et al. IL-34 and CSF-1 display an equivalent macrophage differentiation ability but a different polarization potential. Sci Rep 2018;8:256.

22.   Liu Y, Liu H, Zhu J, Bian Z. Interleukin-34 drives macrophage polarization to the M2 phenotype in autoimmune hepatitis. Pathol Res Pract 2019;215:152493.

23.   Wang B, Tang Y, Sun X, Ouyang X, Li H, Wei J, et al. Increased IL-6 expression on THP-1 by IL-34 stimulation up-regulated rheumatoid arthritis Th17 cells. Clin Rheumatol 2018;37:127-137.

24.   Bezie S, Picarda E, Ossart J, Tesson L, Usal C, Renaudin K, et al. IL-34 is a Treg-specific cytokine and mediates transplant tolerance. J Clin Invest 2015;125:3952-64.

25.   Baghdadi M, Umeyama Y, Hama N, Kobayashi T, Han N, Wada H, et al. Interleukin-34, a comprehensive review. Journal of Leukocyte Biology 2018;104:931-951.

26.   Alexander CM, Reichsman F, Hinkes MT, Lincecum J, Becker KA, Cumberledge S, et al. Syndecan-1 is required for Wnt-1-induced mammary tumorigenesis in mice. Nature Genetics 2000;25:329-32.

27.   Teng YH, Aquino RS, Park PW. Molecular functions of syndecan-1 in disease. Matrix Biol 2012;31:3-16.

28.   Arnett FC, Edworthy SM, Bloch DA, McShane DJ, Fries JF, Cooper NS, et al. The American Rheumatism Association 1987 revised criteria for the classification of rheumatoid arthritis. Arthritis and Rheumatism 1988;31:315-324.

29.   Pickens SR, Chamberlain ND, Volin MV, Pope RM, Mandelin AM, 2nd, Shahrara S. Characterization of CCL19 and CCL21 in rheumatoid arthritis. Arthritis Rheum 2011;63:914-22.

30.   Pickens SR, Chamberlain ND, Volin MV, Pope RM, Talarico NE, Mandelin AM, 2nd, et al. Characterization of interleukin-7 and interleukin-7 receptor in the pathogenesis of rheumatoid arthritis. Arthritis Rheum 2011;63:2884-93.

31.   Kim SJ, Chang HJ, Volin MV, Umar S, Van Raemdonck K, Chevalier A, et al. Macrophages are the primary effector cells in IL-7-induced arthritis. Cell Mol Immunol 2020;17:728-740.

32.   Umar S, Palasiewicz K, Van Raemdonck K, Volin MV, Romay B, Amin MA, et al. IRAK4 inhibition: a promising strategy for treating RA joint inflammation and bone erosion. Cell Mol Immunol 2020.

33.   Van Raemdonck K, Umar S, Palasiewicz K, Volkov S, Volin MV, Arami S, et al. CCL21/CCR7 signaling in macrophages promotes joint inflammation and Th17-mediated osteoclast formation in rheumatoid arthritis. Cell Mol Life Sci 2020;77:1387-1399.

34.   Chang SH, Choi BY, Choi J, Yoo JJ, Ha YJ, Cho HJ, et al. Baseline serum interleukin-34 levels independently predict radiographic progression in patients with rheumatoid arthritis. Rheumatol Int 2015;35:71-9.

35.   Segaliny AI, Brion R, Mortier E, Maillasson M, Cherel M, Jacques Y, et al. Syndecan-1 regulates the biological activities of interleukin-34. Biochim Biophys Acta 2015;1853:1010-21.

36.   Fears CY, Woods A. The role of syndecans in disease and wound healing. Matrix Biol 2006;25:443-56.

37.   Palaiologou M, Delladetsima I, Tiniakos D. CD138 (syndecan-1) expression in health and disease. Histol Histopathol 2014;29:177-89.

38.   Rousseau C, Ferrer L, Supiot S, Bardies M, Davodeau F, Faivre-Chauvet A, et al. Dosimetry results suggest feasibility of radioimmunotherapy using anti-CD138 (B-B4) antibody in multiple myeloma patients. Tumour Biol 2012;33:679-88.

39.   Patterson AM, Cartwright A, David G, Fitzgerald O, Bresnihan B, Ashton BA, et al. Differential expression of syndecans and glypicans in chronically inflamed synovium. Ann Rheum Dis 2008;67:592-601.

40.   Salminen-Mankonen H, Saamanen AM, Jalkanen M, Vuorio E, Pirila L. Syndecan-1 expression is upregulated in degenerating articular cartilage in a transgenic mouse model for osteoarthritis. Scand J Rheumatol 2005;34:469-74.

41.   Kong Y, Wang W, Zhang C, Wu Y, Liu Y, Zhou X. Cannabinoid WIN55,2122 mesylate inhibits ADAMTS4 activity in human osteoarthritic articular chondrocytes by inhibiting expression of syndecan1. Mol Med Rep 2016;13:4569-76.

42.   Ushach I, Zlotnik A. Biological role of granulocyte macrophage colony-stimulating factor (GM-CSF) and macrophage colony-stimulating factor (M-CSF) on cells of the myeloid lineage. Journal of Leukocyte Biology 2016;100:481-9.

43.   Asahara H, Hasunuma T, Kobata T, Inoue H, Muller-Ladner U, Gay S, et al. In situ expression of protooncogenes and Fas/Fas ligand in rheumatoid arthritis synovium. J Rheumatol 1997;24:430-5.

44.   Pap T, Nawrath M, Heinrich J, Bosse M, Baier A, Hummel KM, et al. Cooperation of Ras- and c-Myc-dependent pathways in regulating the growth and invasiveness of synovial fibroblasts in rheumatoid arthritis. Arthritis Rheum 2004;50:2794-802.

45.   Roivainen A, Soderstrom KO, Pirila L, Aro H, Kortekangas P, Merilahti-Palo R, et al. Oncoprotein expression in human synovial tissue: an immunohistochemical study of different types of arthritis. Br J Rheumatol 1996;35:933-42.

46.   Liu L, Lu Y, Martinez J, Bi Y, Lian G, Wang T, et al. Proinflammatory signal suppresses proliferation and shifts macrophage metabolism from Myc-dependent to HIF1alpha-dependent. Proc Natl Acad Sci U S A 2016;113:1564-9.

47.   Park-Min KH. Metabolic reprogramming in osteoclasts. Semin Immunopathol 2019;41:565-572.

48.   Izquierdo E, Cuevas VD, Fernandez-Arroyo S, Riera-Borrull M, Orta-Zavalza E, Joven J, et al. Reshaping of Human Macrophage Polarization through Modulation of Glucose Catabolic Pathways. J Immunol 2015;195:2442-51.

49.   Zhou J, Sun X, Zhang J, Yang Y, Chen D, Cao J. IL-34 regulates IL-6 and IL-8 production in human lung fibroblasts via MAPK, PI3K-Akt, JAK and NF-kappaB signaling pathways. Int Immunopharmacol 2018;61:119-125.

50.   Nandi S, Cioce M, Yeung YG, Nieves E, Tesfa L, Lin H, et al. Receptor-type protein-tyrosine phosphatase zeta is a functional receptor for interleukin-34. Journal of Biological Chemistry 2013;288:21972-86.

51.   Franze E, Dinallo V, Rizzo A, Di Giovangiulio M, Bevivino G, Stolfi C, et al. Interleukin-34 sustains pro-tumorigenic signals in colon cancer tissue. Oncotarget 2018;9:3432-3445.
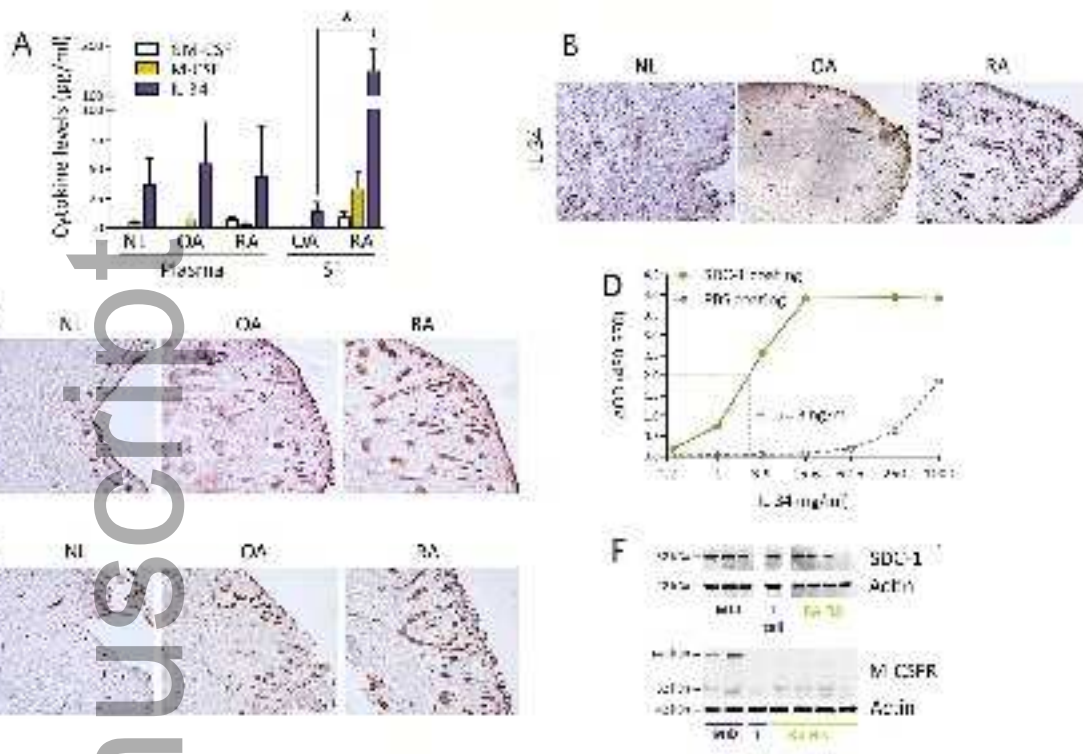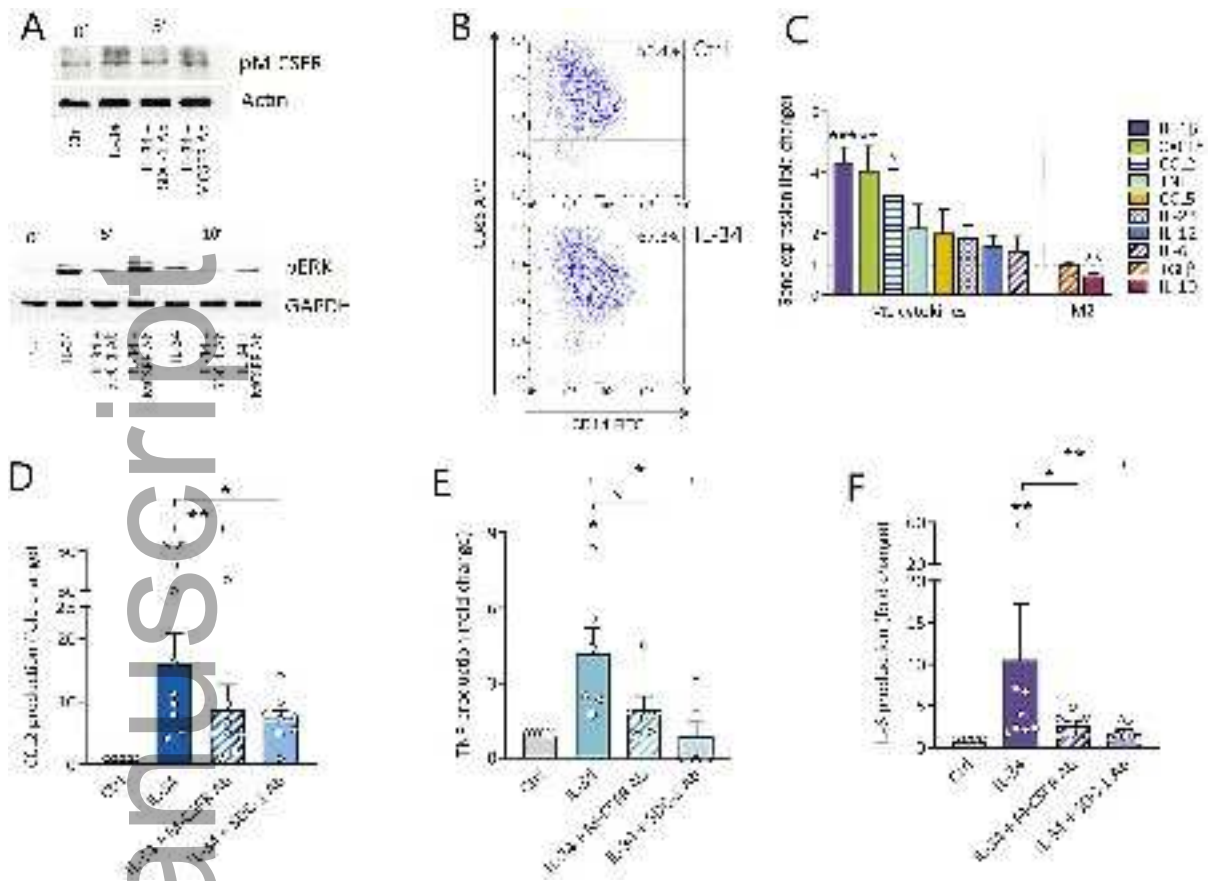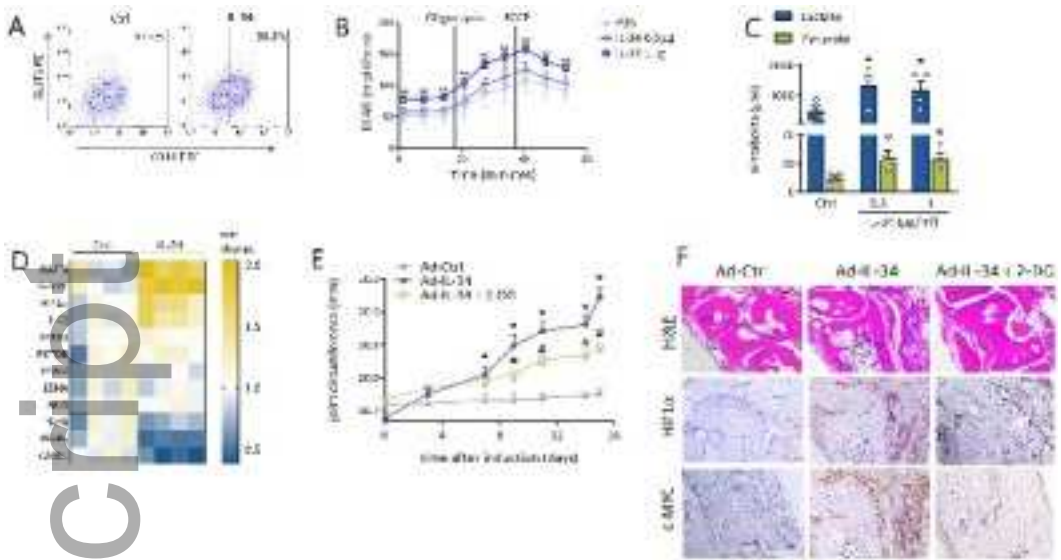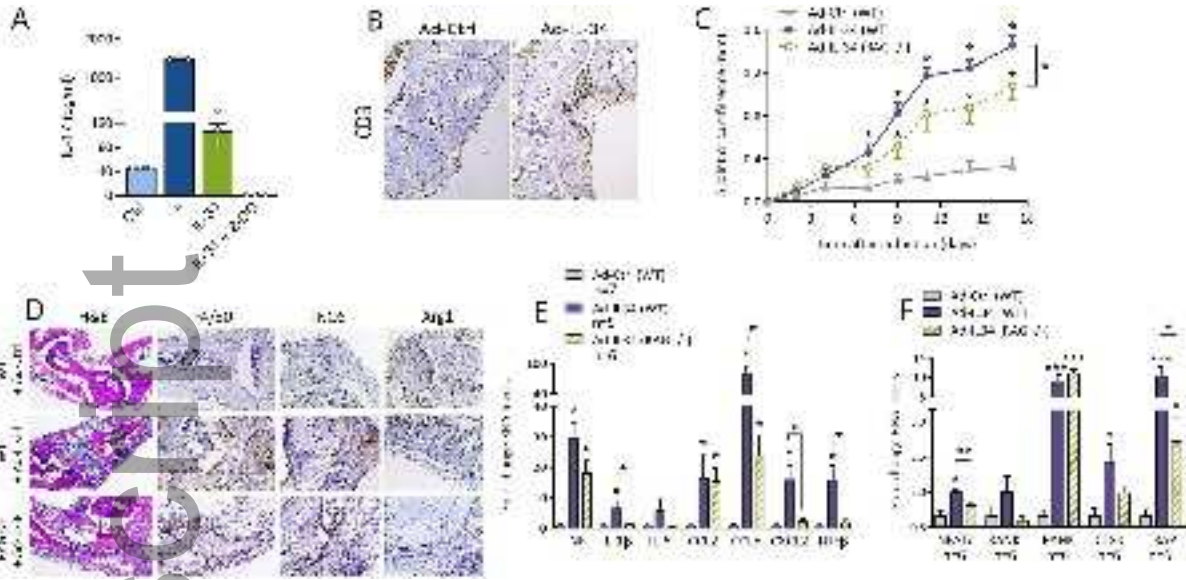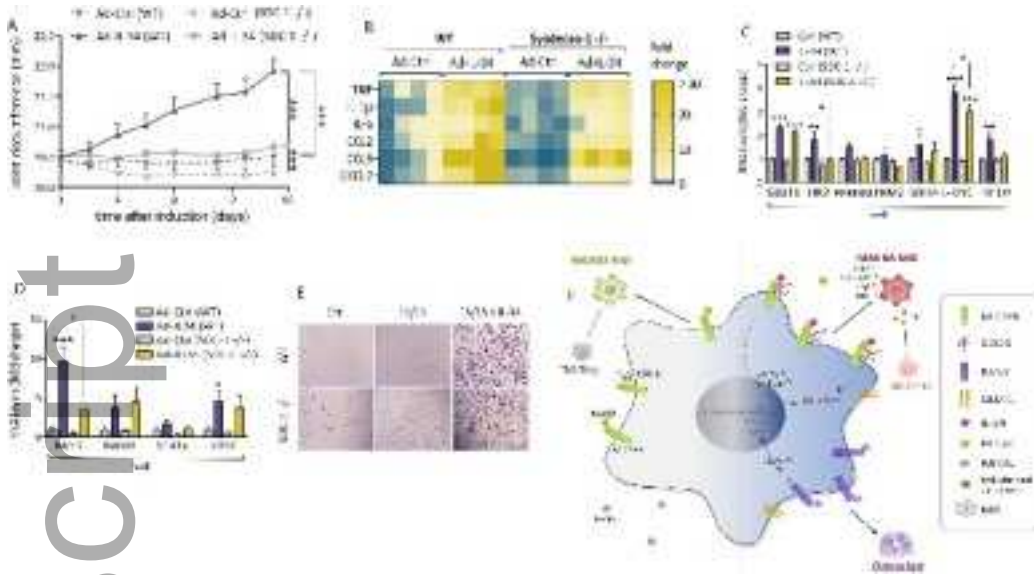
art_41792_f1.tif
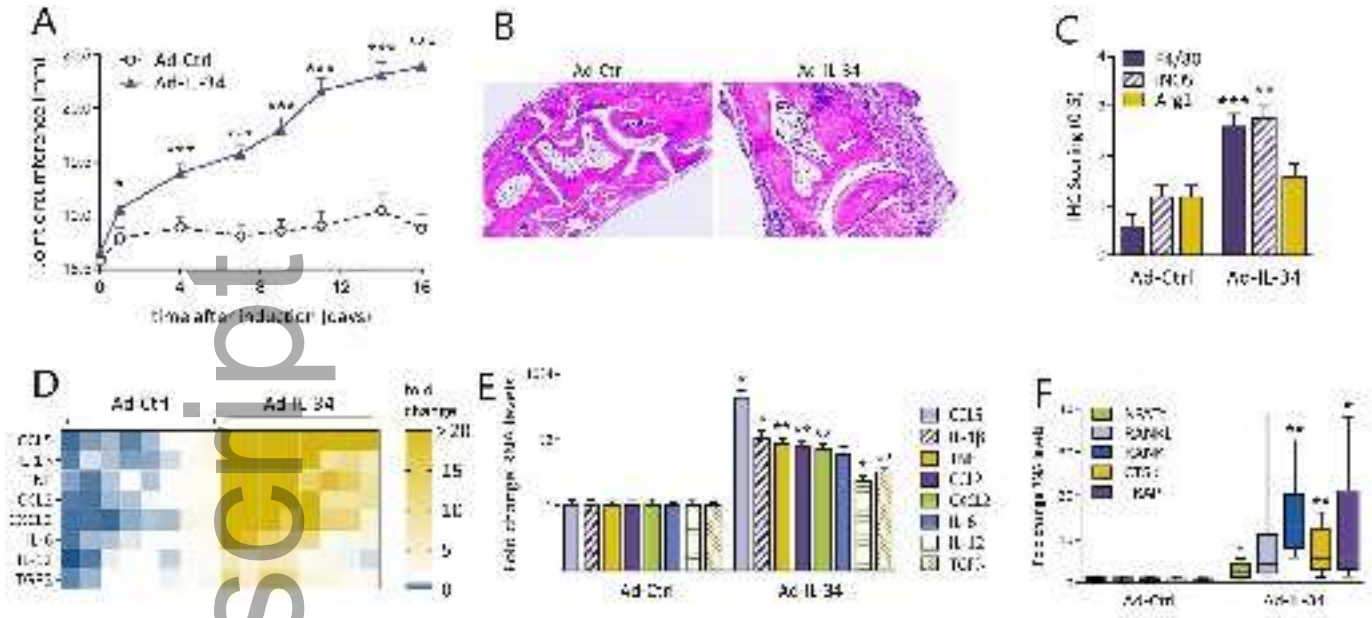
art_41792_f2.tif

art_41792_f3.tiff

art_41792_f4.tif

art_41792_f5.tif

art_41792_f6.tif